Assessing the susceptibility of gap-graded soils to internal erosion: proposition of a new experimental methodology

Didier Marot, Abdul Rochim, Hong-Hai Nguyen, Fateh Bendahmane & Luc Sibille

ONLINE FIRST

 Springer

 Springer

Springer

CrossMark

ORIGINAL PAPER

Assessing the susceptibility of gap-graded soils to internal erosion: proposition of a new experimental methodology

Didier Marot[1] · Abdul Rochim[1,2] · Hong-Hai Nguyen[3] · Fateh Bendahmane[1] · Luc Sibille[4]

Abstract Suffusion and global backward erosion are two of the main internal erosion processes in earth structures and their foundations which may increase their failure risk. For other processes of internal erosion, different classifications exist in order to evaluate the soil erodibility, whereas in the case of suffusion and global backward erosion, no susceptibility classification is available. The absence of suffusion susceptibility classification may be due to the complexity of this process, which appears as the result of the coupled processes: detachment–transport–filtration of a part of the finest fraction within the porous network. Twelve soils, covering a large range of erodibility are tested with a specific triaxial erodimeter. Different criteria based on particle size distribution are compared in order to identify the potential susceptibility to suffusion. For the susceptibility characterization, a new energy-based method is proposed. This method can be used for cohesionless soils and clayey sand, and a single classification is obtained for suffusion tests realized under flow rate-controlled conditions or by increasing the applied hydraulic gradient. For several tests performed on a mixture of kaolinite and sand, suffusion of clay is accompanied by a global backward erosion process. Characterization of the development of clayey sand backward erosion is also addressed by this method. Finally, a complete methodology is detailed for the suffusion and global backward erosion susceptibility characterization.

Keywords Dam safety · Embankment · Internal erosion · Suffusion · Triaxial erodimeter · Flow energy

✉ Didier Marot
didier.marot@univ-nantes.fr

1   Institut de Recherche en Génie Civil et Mécanique, Université de Nantes, 58 Rue Michel Ange, BP 420, 44606 Saint-Nazaire Cedex, France

2   Civil Engineering Department, Sultan Agung Islamic University, Semarang, Indonesia

3   University of Science and Technology, The University of Danang, 54 Nguyen Luong Bang Street, Lien Chieu District, Da Nang City, Vietnam

4   Université Grenoble Alpes, CNRS, 3SR, 38000 Grenoble, France

🖄 Springer

1 Introduction

For the safety of dams and dikes made of soils, internal erosion is a widely present issue in civil and environmental engineering. The complex phenomenon of suffusion is one of the main internal erosion processes (Fell and Fry 2013). It corresponds to the process of detachment and then transport of the finest soil particles within the porous network constituted by the soil itself. However, a fraction of the detached particles can re-settle or be filtered at the bulk of the porous network. This process can eventually induce local clogging. The processes of detachment, transport and filtration of fine particles are thus inseparable. It is worth noting that suffusion process is conditioned by the evolving and interdependent characteristics of the fluid phase as well as the solid phase. Therefore, its study is a complex matter as the phenomenon of suffusion depends on the geometry of the porous medium and also on the physicochemical characteristics of medium and interstitial fluid. Garner and Fannin (2010) describe the main initiation conditions for suffusion with the aid of a diagram comprising three components: material susceptibility, critical hydraulic load and the critical stress condition. In the same manner, Fell and Fry (2013) describe three criteria which have to be satisfied for suffusion to occur: geometric criterion, stress criterion and hydraulic criterion.

Suffusion may cause changes in porosity and can also lead to important modifications in the hydraulic and mechanical characteristics of the soil (Marot et al. 2009; Chang and Zhang 2013a; Ke and Takahashi 2012; Moffat et al. 2011 among others). Moreover, modifications of the porous medium can be the catalyst for slope instability at the scale of hydraulic embankments (Fry et al. 2012). Thus, the suffusion sensibility of embankment soils needs to be characterized to ensure the safety assessment of these structures.

In literature, several soil sensibility classifications were proposed for concentrated leak erosion and scour (Wan and Fell 2004; Hanson and Simon 2001; Briaud 2008; Marot et al. 2011a), whereas erodibility classifications for suffusion and backward erosion are not yet well established.

This paper describes a new methodology for characterizing the suffusion and global backward erosion susceptibility of soils. The comparison of grain size distribution criteria defined in literature permits to identify the less conservative criterion according to the type of grain size distribution. By using the corresponding criterion, it is possible to determine if the tested soil is potentially susceptible to suffusion. For a soil potentially susceptible to suffusion, the corresponding erodibility has to be defined by performing suffusion tests with a dedicated device. The results of an experimental campaign of erosion tests are discussed in terms of ability to define the degree of suffusion susceptibility for several soils which cover a large range of erodibility.

2 A physics-based understanding

## 2.1 Influence of the geometry of the porous medium

The detachment of fine particles and their subsequent transport throughout the porous network of the soil requires that sizes of constriction are sufficiently large. These constriction sizes are conditioned by the granular distribution, but depend also on the grain shape and the density of the granular packing.

Three main gradation curves can be distinguished (Lafleur et al. 1989): linear distribution (curves 1 and 2 in Fig. 1), discontinuous distribution (curve 3) and finally, upwardly concave distribution (curve 4).

In the case of curve 2, the fine particles are uniformly distributed and very few coarse particles float within the fine fraction. In the case of discontinuous distribution, a series of intermediary size grains is missing. The concave distribution consists of a poorly graded coarser fraction associated to a highly graded fine fraction. In this type of soil, the volume between the grains of the coarser fraction is higher than the volume of fine particles, thus enabling the fine particles to migrate. The soils whose grain size distribution curve corresponds to curves 1 or 2 are generally stable to suffusion (Lafleur et al. 1989). The soils that are likely to suffer from suffusion are, according to Fell and Fry (2007), "internally unstable," i.e., their grain size distribution curve is either discontinuous (curve 3) or upwardly concave (curve 4).

In 1981, Kovacs proposed to compute the diameter of the average pore by using a shape coefficient whose values rang between 6 for the spherical particles and up to 7 and 9 for the more angular particles. By using a triaxial erodimeter, Marot et al. (2012) determined the suffusion susceptibility of three mixtures of kaolin aggregates (mixtures with 10 % of kaolin). Results clearly demonstrate that suffusion process depends on the grain angularity of the coarse fraction. With a same grain size distribution, angularity of coarse fraction grains contributes to increase the suffusion resistance. Thus, shape of grains appears as a key parameter of seepage flow in porous media.

For the same granular distribution, the modification of the effective stress can induce grain rearrangements. Several tests performed in oedometric conditions on unstable soils showed that a rise in the effective stress causes an increase in the soils' resistance to suffusion (Moffat and Fannin 2006). In the same manner, when tests were carried out under isotropic confinement (Bendahmane et al. 2008), the increase in the confinement pressure allowed a decrease in the suffusion rate. On the contrary, for a given initial porosity, Chang and Zhang (2013a) showed that the increase in deviatoric stress is linked to an increase in the maximum erosion rate.
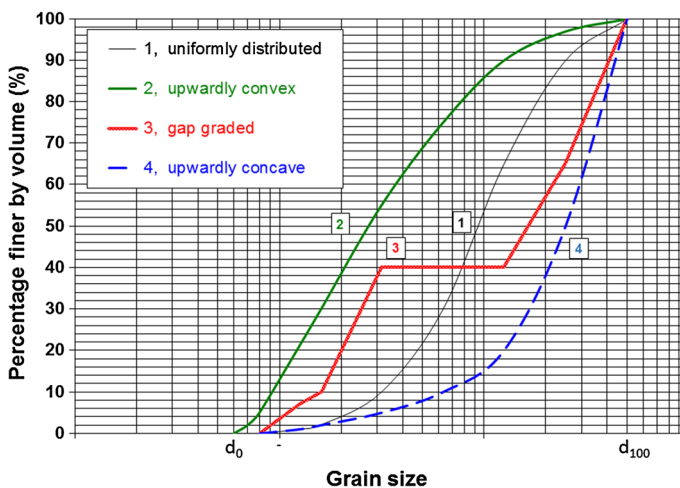
Fig. 1 Main types of gradation curve (after Lafleur et al. 1989)

Suffusion can be described as the result of the process of surface erosion, the surface is here the surface of the pores (Bonelli and Marot 2011), but the fate of detached particles may govern the development of suffusion process (Reddi et al. 2000). The conditions for the evacuation of the detached particles are central points to study filter efficiency, geotextile materials or layers of draining soil. For cohesionless soils, Lafleur (1999) identifies the ideal diameter d_i of the opening of the filter, by starting from the uniformity coefficient and from the aspect of the grain size distribution curve. Depending on the real opening O_F of the pores of a filter, several phenomena can be observed: suffusion, if $O_F \gg d_i$, clogging if $O_F \ll d_i$ and self-filtration if $O_F \approx d_i$. Even if a filter allows the migration of all the fine particles, the constriction size of the filter constitutes a parameter that can influence significantly the initiation and the development of suffusion. When testing suffusion on clayey sands, replacing a filter with a 4 mm opening by filter of a 0.08 mm opening has enabled to rise by 6 the hydraulic gradient required to initiate the clay suffusion (Marot et al. 2009).

3 Determination of the potential susceptibility to suffusion

As the study of suffusion is a complex matter, a first study can consist of evaluating the potential susceptibility to suffusion by taking into account only the grain size distribution. Based on this information, several criteria have been proposed in literature, and three main studies were performed in order to compare the obtained results with such criteria.

According to Li and Fannin (2008), the criteria proposed by Kézdi on the one hand, and Kenney and Lau on the other hand are similar because both methods require an evaluation of the slope of the gradation curve. The authors draw the following conclusions: the two criteria converge for $F = 15$ % (with F the mass percentage of the grains with a size lower than a given particle diameter d). In the case of gap-graded soils, Kézdi's criterion seems to be more suitable for distinguishing stable soils from unstable ones. For the soils with continuous grain size distribution, Kézdi's criterion is more conservative for $F < 15$ % and conversely, Kenney and Lau's criterion is more conservative for $F > 15$ %. This comparison of criteria is only relevant for cohesionless soils.

Wan and Fell (2008) have carried out 20 suffusion tests on mixtures of clay–silt–sand–gravel and silt–sand–gravel mixtures. Three criteria were used for predicting the initiation of suffusion: the Sherard's criterion, the Kenney and Lau's criterion and Burenkova's criterion. They concluded that these methods, based on particle size distribution are conservative and they proposed a method for assessing internal instability of broadly graded silt–sand–gravel soils. This method is based on two ratios: d_{90}/d_{60} and d_{20}/d_5 (where d_{90}, d_{60}, d_{20} and d_5 are the sieve sizes for which 90, 60, 20 and 5 % respectively of the weighed soil is finer). According to the authors, this method seems not to be applicable for gap-graded soils and soils with a mass of fine fraction lower than 15 %.

Chang and Zhang (2013b) propose three categories of soil erodibility from the comparison of criteria proposed by Istonima, Kézdi and Kenney and Lau. They defined P as the mass fraction of particles finer than 0.063 mm. For gap-graded soil, Chang and Zhang defined the gap ratio as: $G_r = d_{max}/d_{min}$ (d_{max} and d_{min}: maximal and minimal particle sizes characterizing the gap in the grading curve). For P less than 10 %, the authors assumed that the stability is correctly assessed using the criterion $G_r < 3$. For P higher than 35 %, the gap-graded soil is reputed stable, and with P in the range 10–35 % the soil is stable if $G_r < 0.3P$. According to Chang and Zhang, their method is only applicable to low-plasticity soils.

4 Characterization of suffusion susceptibility

4.1 Introduction

It is worth stressing that grain size distribution criteria don't take into account several important parameters such as: the mineralogy of the material, the shape of the grains, the soil density and the effective stress. Finally, even if the transport of particles is geometrically feasible, the action of the hydraulic flow must be sufficient to detach soil particles. Thus, Kovacs (1981) recognized that even if the geometrical conditions allow particle movements, the hydraulic conditions have to be studied.

4.2 Hydraulic criteria

The hydraulic loading on the grains is often described by three distinct parameters characterizing the hydraulic loading: the hydraulic gradient, the hydraulic shear stress and the pore velocity. However, the filtration of some detached particles can induce a clogging process within the soil accompanied with the decrease in the hydraulic conductivity (Reddi et al. 2000; Bendahmane et al. 2008; Marot et al. 2009; 2011b; Nguyen et al. 2012; Luo et al., 2013). Therefore, variations of both seepage velocity and hydraulic gradient (or pressure gradient) have to be taken into account to evaluate the hydraulic loading.

Reddi et al. (2000) proposed to represent the porous medium by a system of parallel capillary tubes each of a constant radius r. Assuming that hydraulic loading can be represented by a shear stress, the latter is given for a horizontal flow between an upstream section A and a downstream section B of the system by:

$$\tau = \left(\frac{\Delta P}{\Delta L}\right)\frac{r}{2} \tag{1}$$

where $\Delta P = P_A - P_B$ is the pressure drop between sections A and B, ΔL is the distance between sections A and B and $r = d_0/2$ with d_0 the average pore diameter in coarse fraction defined by Kovacs (1981).

The expression of hydraulic shear stress can be reformulated in the case of a vertical flow by the equation:

$$\tau = \left(\frac{\Delta h \gamma_w}{\Delta z}\right)\frac{r}{2} \tag{2}$$

where Δh is the drop of hydraulic head between sections A and B, $\Delta z = z_A - z_B$, z_A and z_B are altitudes of sections A and B respectively, and γ_w is the unit weight of water. It is worth stressing that such approach leads to the same expression of hydraulic shear stress as expression proposed by Wörman and Olafsdottir (1992).

In the case of cohesive soils, Reddi et al. (2000) proposed to estimate the typical radius of pores by:

$$r = \sqrt{\frac{8K}{n}} \tag{3}$$

where n is the porosity and K the intrinsic permeability determined by:

$$K = k\frac{\eta}{\gamma_w} \tag{4}$$

with k the hydraulic conductivity, η the dynamic viscosity.

Consequently, the hydraulic shear stress along vertical system of capillary tubes can be expressed by:

$$\tau = \left(\frac{\Delta h}{\Delta z}\right)\sqrt{\frac{2k\eta\gamma_w}{n}} \tag{5}$$

It is worth noting that in Eq. (5), changes of both hydraulic head drop and permeability during the erosion process are considered.

From results of hole erosion tests and jet erosion tests, Marot et al. (2011a) proposed a new analysis based on the energy expended by the seepage flow which is a function of both the flow rate and the pressure gradient. Three assumptions were used: the fluid temperature is assumed constant, the system is considered as adiabatic and only a steady state is considered. The energy conservation equation permits to express the total flow power as the summation of the power transferred from the fluid to the solid particles and the power dissipated by viscous stresses in the bulk. As the transfer appears negligible in suffusion case (Sibille et al. 2015a), the authors suggest to characterize the fluid loading from the total flow power, P_{flow} which is expressed by:

$$P_{\text{flow}} = (\gamma_w \Delta z + \Delta P)Q \tag{6}$$

where Q is the fluid flow rate.

$\Delta z > 0$ if the flow is in downward direction, $\Delta z < 0$ if the flow is upward and the erosion power is equal to $Q\Delta P$ if the flow is horizontal.

The expended energy E_{flow} is the time integration of the instantaneous power dissipated by the water seepage for the test duration.

4.3 Erosion susceptibility classifications

Concerning erosion susceptibility classification, three methods were proposed in the case of scour and concentrated leak erosion. The two first methods were proposed by Hanson and Simon (2001) in the case of use of jet erosion tests and by Wan and Fell (2004) for hole erosion tests. For these methods, authors assume a linear relation between the rate of erosion $\dot{m}$ per unit surface, and the hydraulic shear stress:

$$\dot{m} = k_d(\tau - \tau_c) \quad \text{if } \tau \geq \tau_c \tag{7}$$

where k_d is the erosion rate coefficient, τ is the hydraulic shear stress and τ_c is the critical shear stress below which erosion is not triggered.

According to values of both k_d coefficient and critical shear stress τ_c, Hanson and Simon (2001) proposed five categories of soil erodibility between very resistant to very erodible. Wan and Fell (2004) proposed six categories varying from extremely slow to extremely rapid erosion with respect to the value of the erosion rate index I_{kd} determined by:

$$I_{kd} = -\log(k_d) \tag{8}$$

The third method (Marot et al. 2011a) is based on an erosion resistance index as:

$$I_\alpha = -\log\left(\frac{\text{Eroded dry mass}}{E_{\text{flow}}}\right) \tag{9}$$

Depending on the values of I_α index, six categories of soil erodibility were proposed from highly erodible to highly resistant.

However, these classifications only concern the cases of concentrated leak erosion and scour; suffusion erodibility classification and also global backward erosion classification are not yet well established.

5 Discussion

5.1 Identification of the less conservative criteria for potential susceptibility to suffusion

From the comparisons of criteria realized by Li and Fannin (2008), Wan and Fell (2008) and Chang and Zhang (2013b), the following conclusions can be drawn:

1. In the case of gap-graded soils and if the percentage of fine particles is higher than 35 %, soil seems to be stable.
2. For gap-graded soils with a fine content less than 35 %, Chang and Zhang's criterion seems to be the less conservative.
3. For widely graded soils, the fine fraction is identified within the granular distribution by the minimum value of Kenney and Lau's ratio $(H/F)_{min}$. If the percentage of fine particles is lower than 15 % and the soil non-plastic, the evaluation of susceptibility can be determined by Kenney and Lau's criterion. For a higher percentage of fine particles, the susceptibility is evaluated by Wan and Fell's criterion. A comparison with Chang and Zhang's criterion must be also realized as this criterion defines the fine content not by the ratio $(H/F)_{min}$ but by the percentage finer than 0.063 mm.

5.2 Specific device for erodibility characterization

A triaxial erodimeter was designed to apply downward seepage flow on intact fine soil samples or on reconstituted fine soil specimens (50 mm in diameter and height up to 100 mm) (see Fig. 2). A detailed description of the device is reported in Bendahmane et al. (2008) and a brief summary is provided hereafter.
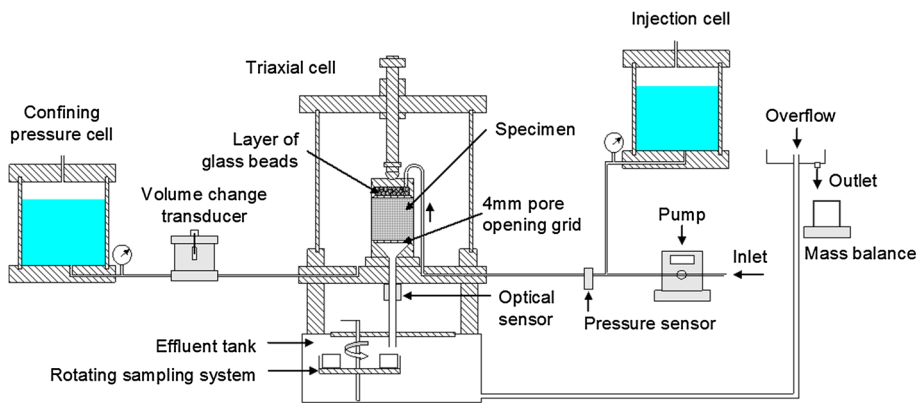
Fig. 2 Schematic diagram of the triaxial erodimeter

The testing device comprises a modified triaxial cell designed to saturate the sample with an upward interstitial flow, to consolidate it under isotropic confinement and finally to force fluid through the sample during the erosion test in the downward direction. The fluid circulates into the top cap which contains a layer of glass beads to diffuse the fluid uniformly on the specimen top surface. The system to generate a seepage flow under a controlled hydraulic gradient comprises an injection cell equipped with pressure sensor, and connected to an air/water interface cylinder. The system to generate seepage flow in flow rate-controlled conditions comprises a gear pump connected to a pressure sensor at its outlet. The funnel-shaped draining system is connected to an effluent tank by a glass pipe. The effluent tank is equipped with an overflow outlet (to control the downstream hydraulic head) and a rotating sampling system containing 8 beakers for the sampling of eroded particles carried out with the effluent. In the case of clay or silt suffusion, a multi-channel optical sensor is placed around the glass pipe (Marot et al. 2011b). Clay or silt concentration in the effluent is computed from the signal sent by the optical sensor and thanks to a calibration of the latter. Fine particle concentration in the effluent is expressed as the ratio of the mass of fine particles to water mass within the fluid. The time integration of the fine particle concentration gives the cumulative eroded dry mass for the corresponding duration (Bendahmane et al. 2008). Moreover, the detection of sand grains in the effluent is assessed from the comparison of the voltages of each LED composing the optical sensor. At the overflow outlet of the effluent tank, water falls in a beaker which is continuously weighed in order to determine injected flow rate. A confining pressure cell connected to an air/water interface cylinder is used to generate the isotropic confinement of the soil sample. Sample volume change is measured by automatic volume change transducer connected between confining pressure cell and the inlet of triaxial cell. The sample is supported by a lower mesh screen, and the mesh screen opening size is selected with the objective to reproduce the situation of an earth structure without filter, as a dike for example.

5.3 Soil properties and test procedure

Twelve soils, composed of clay and sand or composed of sand and gravel, were tested. A laser diffraction particle size analyser was used to measure the grain size distribution of
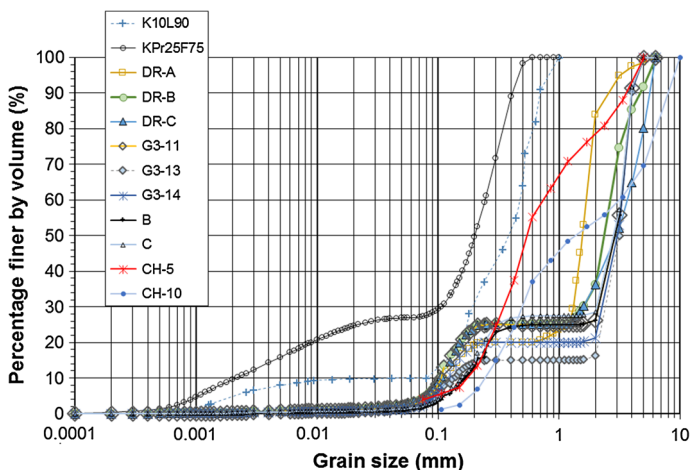
Fig. 3 Grain size distribution of tested soils

these soils (see Fig. 3). Tests were performed with demineralized water and without deflocculation agent.

As the maximum grain diameter of the coarser tested soil (CH-10) is 10 mm, the minimum value of ratio cell diameter to maximum grain diameter is 5 and then higher than in the case of several other internal erosion studies (as for example the study performed by Kenney and Lau 1985).

K10L90 is a mixture of 90 % Loire sand (percentage by weight) and 10 % kaolinite clay (marketed by Prolabo). KPR25F75 is a mixture of 75 % Fontainebleau sand and 25 % kaolinite proclay. Except KPR25F75 mixture, all tested soils can be considered as non-plastic soils, as their liquid limit and plastic limit are about 0. The liquid limit and plastic limit for KPR25F75 are 21 and 14 %, respectively (USCS classification: CL).

The pore opening size of the lower mesh screen is 4 mm in order to permit the erosion of most of the grains, as in an earth structure without any filter.

Table 1 summarizes the soils used in the laboratory tests and their properties. When the methods proposed by Chang and Zhang (2013b), Kenney and Lau (1985) and Wan and Fell (2008) can be applied for considered soils, the potential susceptibility to suffusion is determined according to these criteria. When for a given soil, two or three methods can be applied, identical classifications can be noted for five soils (DR-B, DR-C, G3-11, G3-13 and G3-14). Whereas for five other soils (DR-A, B, C, CH-5, CH-10), the classifications defer depending on the criterion.

For each soil, it is possible to select the less conservative criteria in accordance with the aforementioned identification. The corresponding susceptibility classification based on these geometric criteria is indicated in bold in Table 1. Now, according to the selected criteria, six soils appear unstable (K10L90, DR-B, DR-C, G3-11, G3-13, G3-14) and four soils appear stable (KPr25F75, DR-A, B, C). However, it seems to be more difficult to identify the potential susceptibility to suffusion of soils, CH-10 and CH-5, as Chang and Zhang's criterion on one hand and Wan and Fell's criterion on the other hand lead to an opposite classification.

Two types of specimen preparation methods were used. For the isotropic confinement condition test (8 tests were performed using such conditions), specimens are prepared using a single-layer semi-static compaction technique with a 50 mm diameter and 50 mm high mold. Then, specimens are placed in a membrane and a 15 kPa isotropic confinement pressure is applied. After this step, carbon dioxide is injected followed by the saturation phase which requires approximately 24 h. The last step consists in applying a target value of confining pressure (between 15 and 100 kPa). Fifteen tests were realized without confinement, and they were prepared in identical mold with a membrane between soil and mold. The saturation is realized with the same aforementioned method. Finally, all specimens are subjected to a seepage flow in downward direction with deaerated and demineralized water. Table 2 indicates the initial dry density of specimens, the values of applied hydraulic gradient or injected flow rate, the confining pressure and the duration for each test.

The repeatability of tests was verified by performing two tests in the same conditions: tests DR-C1 and DR-C2.

5.4 Post-test particle size distributions of specimens

With the objective to study the influence of suffusion on the soil gradation, the grain size distribution of a KPR25F75 specimen was measured just after the saturation phase and also at the end of test F14. Figure 4 shows that the suffusion process induces a small decrease in

Table 1 Properties and potential susceptibility classifications based on geometric criteria of soils tested

Soil reference in paper	C_u	G_r	P (%)	d_5 (mm)	d_{20} (mm)	d_{60} (mm)	d_{90} (mm)	$(H/F)_{min}$	$d_{(H/F=min)}$ (mm)	Susceptibility classification		
										Chang and Zhang's criterion	Kenney and Lau's criterion	Wan and Fell's criterion
K10L90	5.92	4.3	10	0.002	0.162	0.473	0.693	0.028	0.019	U	–	–
KP25F75	114.35	WG	27	0.001	0.009	0.245	0.411	0.122	0.020	S	–	–
DR-A	14.91	2.4	1.7	0.094	0.250	1.692	2.633	0.109	0.212	S	U	–
DR-B	26.03	4.8	3.3	0.080	0.151	2.712	4.727	0	0.250	U	U	–
DR-C	35.25	4.8	3.3	0.080	0.151	3.671	5.645	0	0.250	U	U	–
G3-11	30.53	6.0	2.7	0.084	0.153	3.250	3.965	0	0.250	U	U	–
G3-13	25.04	6.0	1.6	0.100	2.127	3.362	3.993	0	0.250	U	U	–
G3-14	29.17	6.0	1.7	0.094	0.250	3.309	3.980	0	0.250	U	U	–
B	19.58	2.5	1.6	0.111	0.261	3.250	3.965	0.035	0.400	S	U	–
C	20.53	2.5	1.7	0.109	0.248	3.217	3.957	0.034	0.400	S	U	–
CH-5	4.25	WG	3	0.094	0.263	0.750	3.629	0.383	1.180	U	S	S
CH-10	12.92	WG	1	0.186	0.368	3.178	8.354	0.406	1.180	U	S	S

C_u uniformity coefficient, G_r gap ratio, WG widely graded soil, P percentage of particle smaller than 0.063 mm, S stable, U unstable; – method not relevant for considered soil

Table 2 Initial dry density, applied hydraulic gradient or injected flow rate, confining pressure and test duration

Soil reference in paper	Specimen reference in paper	Initial dry density (kN/m^3)	Applied hydraulic gradient	Injected flow (ml/min)	Confining pressure (kPa)	Test duration (min)
K10L90		17	2	–	100	31.9
KPR25F75	F14	16	5	–	15	230.0
	F15	16	7	–	15	195.1
	F13	16	10	–	15	286.3
	F10	16	18	–	15	299.5
	F20	16	–	1.2	15	278.4
	F17	16	–	1.4	15	210.5
	F23	16	–	1.6	15	200.2
B	B-q1	17.39	–	1.6	0	270
	B-q2	17.39	–	12	0	210
	B-i1	17.39	From 0.1 to 6	–	0	180
	B-i2	17.39	From 1 to 10	–	0	100
	B-i3	17.39	4	–	0	300
C		17.39	From 0.1 to 7	–	0	190
DR-A		17.87	From 0.1 to 16	–	0	340.2
DR-B		16	From 0.1 to 7	–	0	220.1
DR-C	C1	16	From 0.1 to 7	–	0	220.1
	C2	16	From 0.1 to 7	–	0	220.1
G3-11		16	From 0.1 to 5	–	0	180.6
G3-13		16	From 0.1 to 6	–	0	200.1
G3-14		16	From 0.1 to 8	–	0	240.4
CH-5		16.54	From 0.1 to 14	–	0	320.2
CH-10		16.86	From 0.1 to 9	–	0	260.5
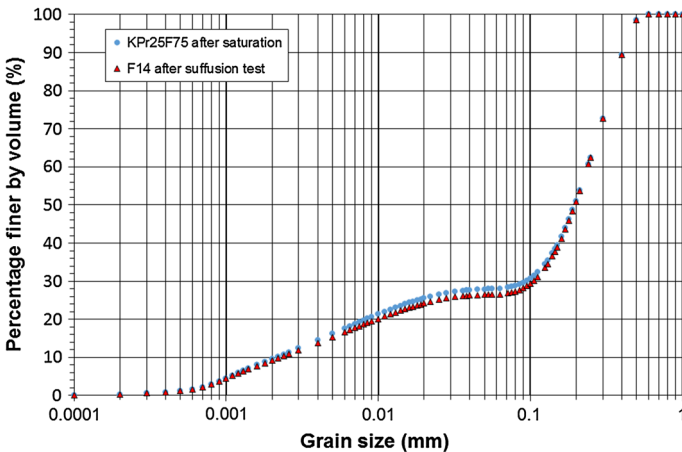
Fig. 4 Grain size distribution of clayey sand KPR25F75, after saturation and after suffusion test F14
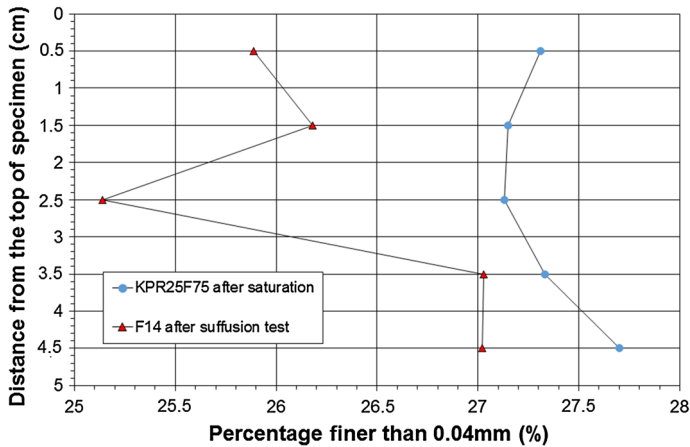
Fig. 5 Vertical profile of percentage finer than 0.04 mm for clayey sand KPR25F75, after saturation and after suffusion test F14

the percentage of fine particles in such clayey sand specimen. Figure 5 underlines that the loss of fine particles appears slightly higher in the upstream part of the specimen.

For tests F10, F17, F20 and F23, first the suffusion of clay was observed during several minutes. The maximum grain diameter of kaolinite proclay is 0.045 mm (grain size distribution measured with a laser diffraction particle size analyser without deflocculation agent), but progressively sand grains could be detected in the effluent thanks to the optical sensor. Figure 6 shows that for the example of test F23, the clay particles represent more than 75 % of eroded particles in the beaker which corresponds to the first 45 min of test, but only 42 % from 45 min to 50 min and finally 34 % from 50 to 55 min of test. It can also be observed that the erosion of sand first only concerns the smallest grains from 0.02 to 0.1 mm. During these tests, the erosion of clay and sand first induced a decrease in the specimen diameter at the bottom and then this volume variation progressed in upward direction. In consequence, this erosion process can be named global backward erosion.

The higher loss of fine particles in the upstream part of the specimen in comparison with downstream specimen part appears also in the case of cohesionless soil B (see Fig. 7).

5.5 Hydraulic behavior of tested specimens

The evolutions with time of the hydraulic conductivity for clayey soils are shown in Fig. 8a and b and in Fig. 9 for cohesionless soils. In Fig. 8a and b, arrows show time detection of sand grains in effluent. For both types of soils, it is worth stressing that the hydraulic conductivity decreases with time when a constant hydraulic gradient is applied (see test K10L90 and tests F10 to F15 in Fig. 8a and test B-i3 in Fig. 9). For tests realized under flow rate-controlled conditions (see tests F17, F20, F23 in Fig. 8b and tests B-q1 and B-q2 in Fig. 9), the hydraulic conductivity decreases, except when the backward erosion starts which leads to the increase in the hydraulic conductivity (tests F17, F20 and F23). Finally, it can be noted that the growth of the applied hydraulic gradient is accompanied by the increase in hydraulic conductivity (see tests C, DR-A, DR-B, DR-C1, DR-C2, G3-11, G3-13, G3-14, CH-5, CH-10, B-i1, B-i2 in Fig. 9).
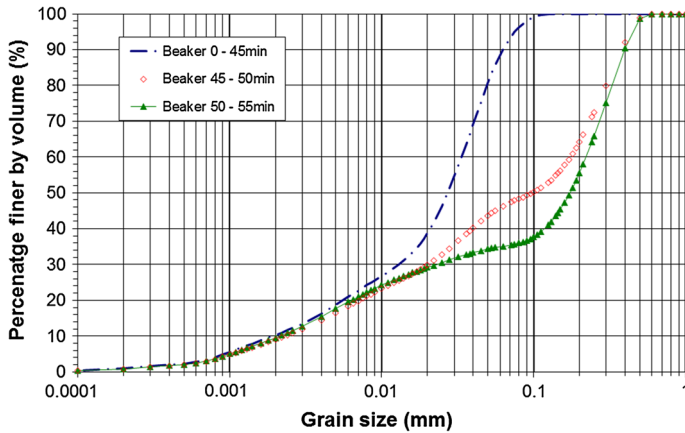
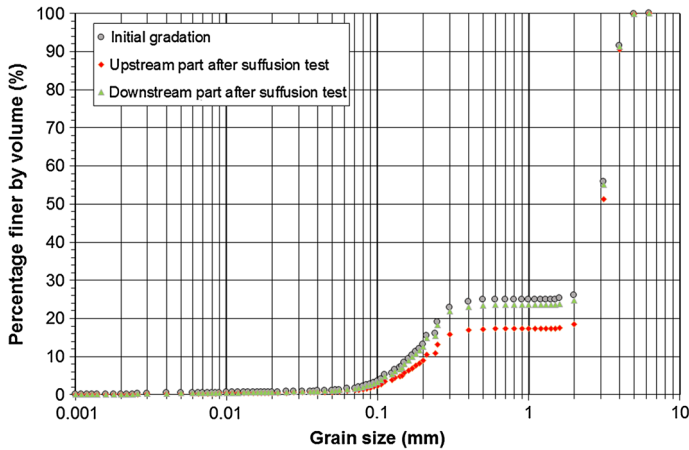**Fig. 6** Grain size distribution of eroded particles, test F23

Fig. 7 Grain size distribution of specimen B-i2, initial gradation, upstream and downstream specimen parts after suffusion test

At the end of each suffusion test, the hydraulic conductivity is relatively constant (in Figs. 8a and 9, black spots show time of stabilization of hydraulic conductivity), except for the case of global backward erosion development which finally leads to the collapse of the specimen.

The hydraulic shear stress is computed by Eq. (5). Figures 10a and b show the hydraulic shear stress evolution during the experiment's duration on cohesive soils, and the corresponding values for cohesionless soils are plotted in Fig. 11.

For both types of soils, under a constant hydraulic gradient, the hydraulic shear stress decreases all along the tests (Tests K10L90, F10, F13, F14, F15, B-i3). The hydraulic shear stress increases during tests F17, F20, F23, B-q1 and B-q2 which were realized under flow rate-controlled conditions and during tests performed with an increasing hydraulic gradient (tests C, DR-A, DR-B, DR-C1, DR-C2, G3-11, G3-13, G3-14, CH-5, CH-10, B-i1, B-i2).
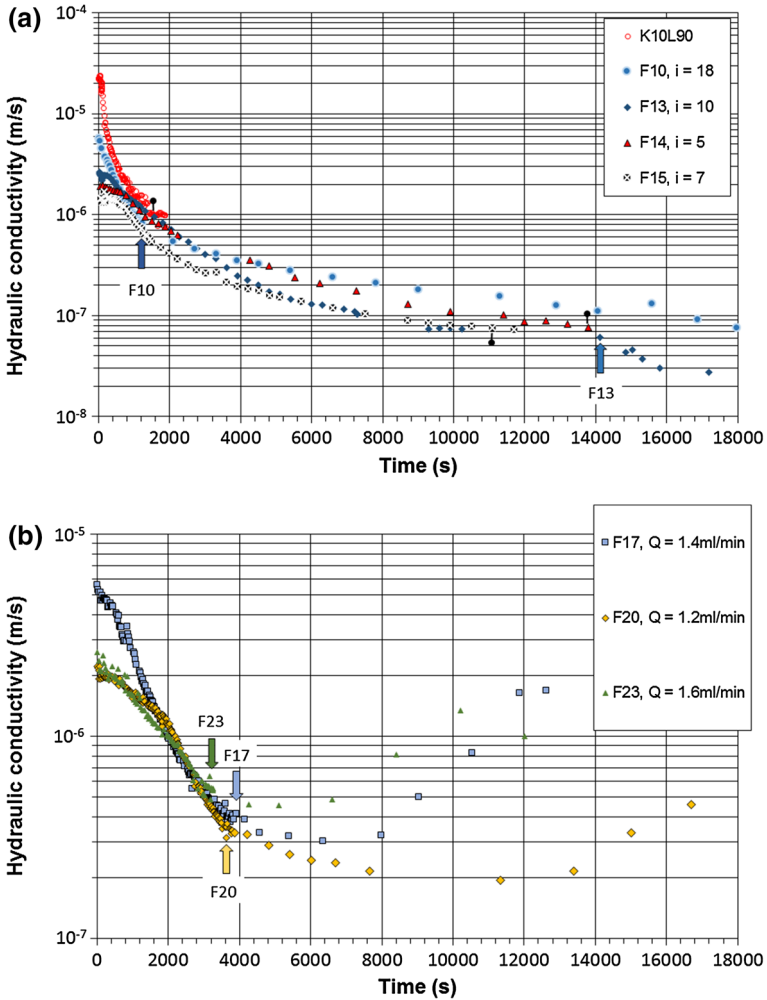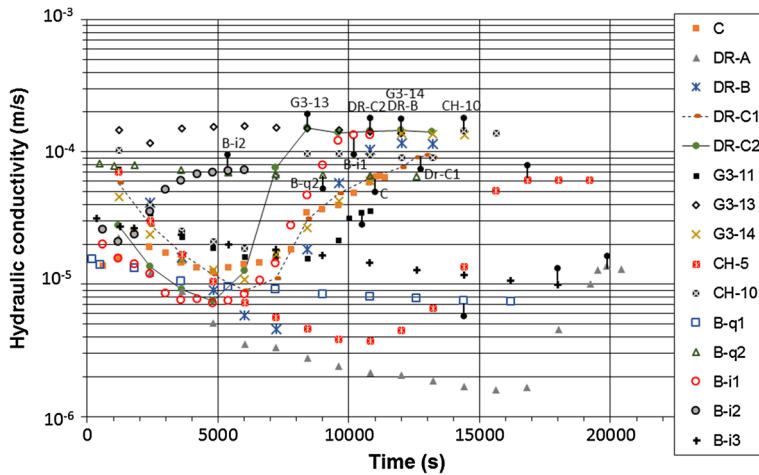
Fig. 8 Hydraulic conductivity vs time for cohesive soils **a** test K10L90, tests F10 to F15; **b** tests F17 to F23. *Arrows* show time detection of sand grains in effluent and *black spots* show time of stabilization of hydraulic conductivity. Applied hydraulic gradient *i* and injected flow rate *Q* are specified for tests F10 to F23

5.6 Proposed method for classification of suffusion sensibility

In conformity with methods proposed by Hanson and Simon (2001) and by Wan and Fell (2004) for scour or concentrated leak erosion classification, a first approach to define a suffusion sensibility classification can consist to investigate the variation of the rate of erosion with the hydraulic shear stress. The rate of erosion is expressed per unit cross section by:

$$\dot{m} = \frac{m_{\text{eroded}}(\Delta t)}{S \Delta t} \tag{10}$$

Fig. 9 Hydraulic conductivity versus time for cohesionless soils. *Black spots* show time of stabilization of hydraulic conductivity

where $m_{eroded}(\Delta t)$ is the mass of eroded particles for the duration Δt, and S is the cross section of the specimen.

Figure 12 shows the rate of erosion versus hydraulic shear stress for cohesive soils, and Fig. 13 shows the corresponding values for cohesionless soils. For each type of soil, the data are plotted in logarithmic scale in order to improve the reading for a large range of data. With the objective to distinguish the two internal erosion processes which appear during tests F10, F13, F17, F20 and F23, data characterizing global backward erosion process are named F10-BE, F13-BE, F17-BE, F20-BE and F23-BE, respectively.

Figure 13 shows that repeatability is fairly good, as representation points are close for tests DR-C1 and DR-C2.

In the case of cohesive soils (Fig. 12), relation following a power law seems to exist between erosion rate and hydraulic shear stress. However, under constant hydraulic gradient, the hydraulic shear stress continuously decreases (test K10L90, tests F10, F13, F14, F15). Thus, such relation characterizes the decrease in suffusion process during the time (i.e., the graph doesn't show the suffusion development, in the contrary of scour erosion or concentrated leak erosion). The linear extrapolation toward a minimum value of hydraulic shear stress will correspond to the end of the suffusion process (i.e., not the threshold of the suffusion initiation). Moreover, the results obtained for tests F10, F13, F17, F20 and F23 realized on the same clayey sand show that global backward erosion can start on a large range of hydraulic shear stress (between 0.023 and 0.165 Pa for tests F13 and F23, respectively).

For cohesionless soils (Fig. 13), a large range of erosion rate can be obtained for a given soil and a given value of hydraulic shear stress. Tests B-q1, B-q2, B-i1, B-i2 and B-i3 realized on a same cohesionless soil reveal that it is not possible to identify precisely a relation of erosion rate with hydraulic shear stress. Thus, such approach is influenced by the applied hydraulic loading history which was different for these tests. This influence of hydraulic loading history was also observed by Luo et al. (2013) who compared the results obtained with two test durations on a sandy gravel. They notably concluded that a long-term large hydraulic head reduces the hydraulic gradient needed for large suffusion
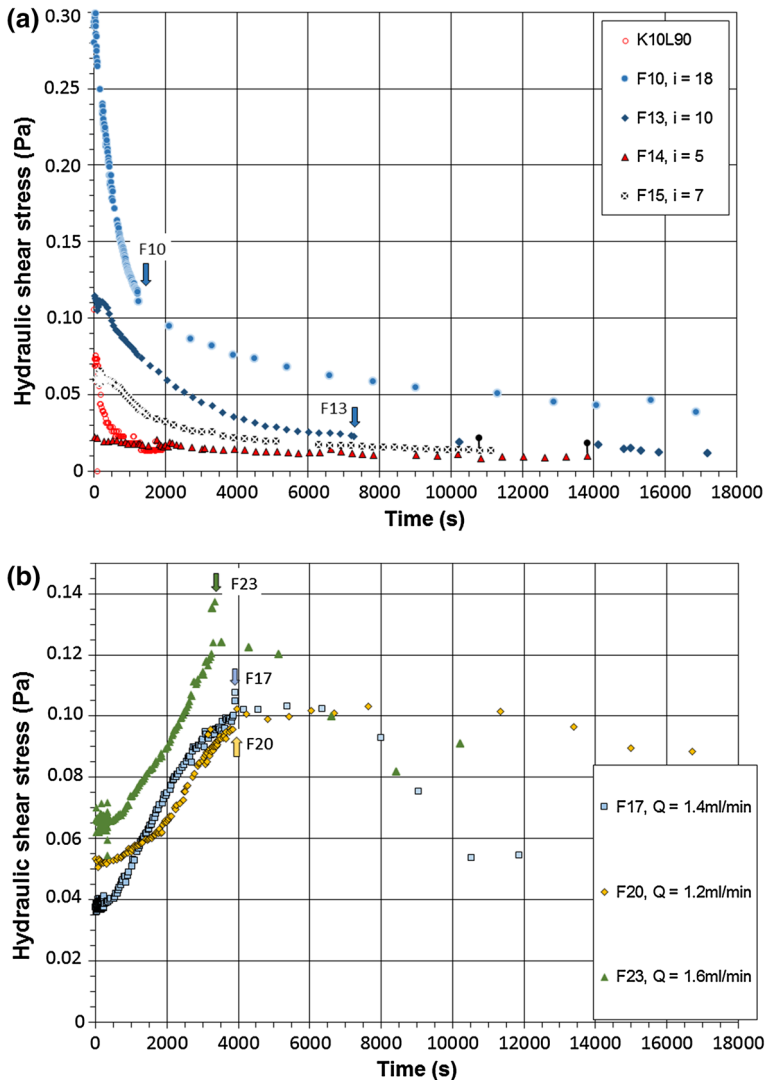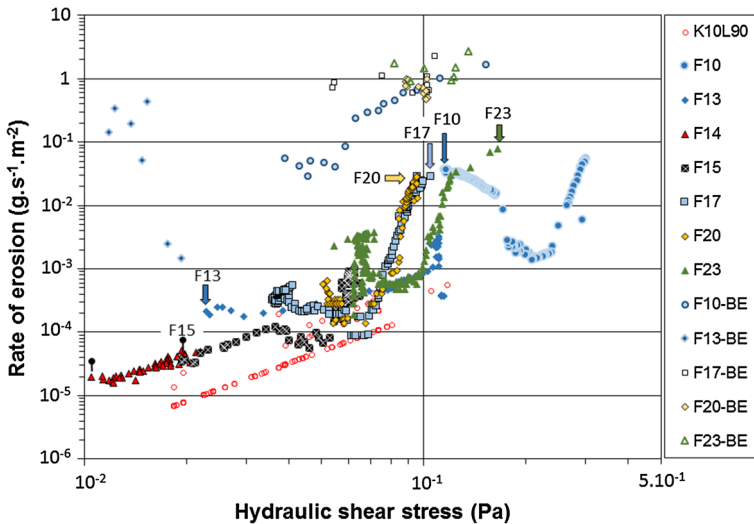
Fig. 10 Hydraulic shear stress versus time, suffusion of cohesive soils **a** test K10L90, tests F10 to F15, **b** tests F17 to F23. *Arrows* show time detection of sand grains in effluent and *black spots* show time of stabilization of the hydraulic conductivity. Applied hydraulic gradient *i* and injected flow rate *Q* are specified for tests F10 to F23

development. Sibille et al. (2015b) tested mixtures of glass beads under multistaged hydraulic gradients. Even if the suffusion of such material induces a slight variation of hydraulic conductivity, Sibille et al. (2015b) showed the necessity to take into account the history of hydraulic loading, i.e., the amplitude but also the duration of each hydraulic gradient stage. With such objective, they expressed the erosion rate as a function of the flow energy per unit volume, which is cumulated from the initiation of each hydraulic stage. Here, for the suffusion susceptibility characterization of several soils under different
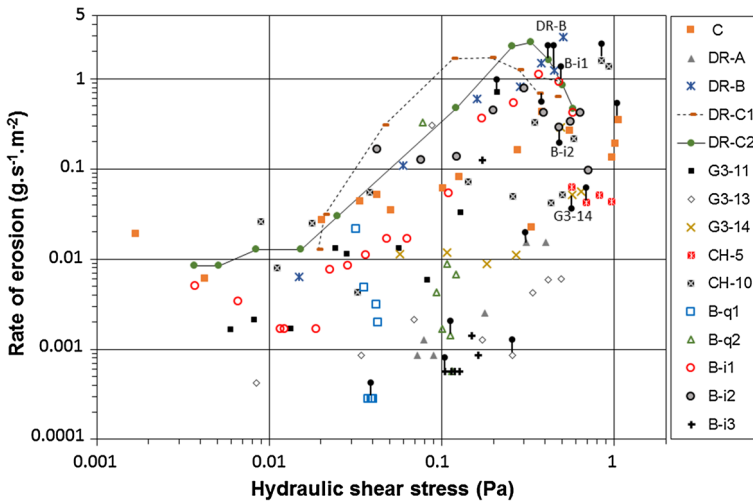
Author's personal copy
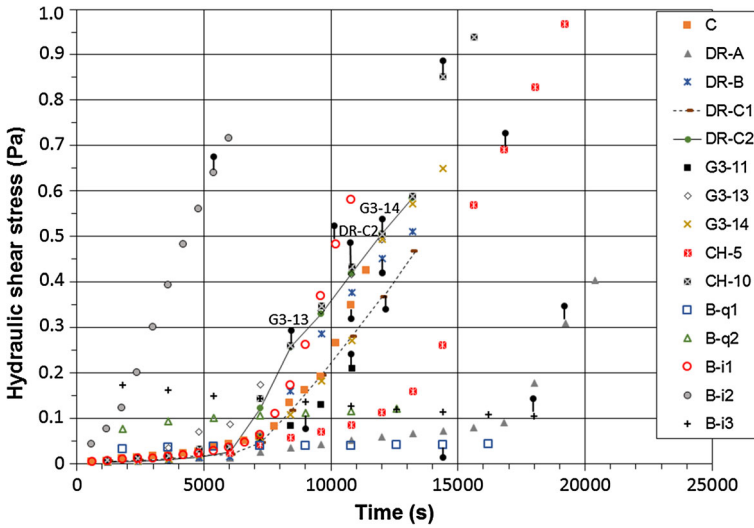
Fig. 11 Hydraulic shear stress versus time, suffusion of cohesionless soils. *Black spots* show time of stabilization of the hydraulic conductivity

Fig. 12 Erosion rate versus hydraulic shear stress, suffusion of cohesive soils. *Arrows* show time detection of sand grains in effluent and *black spots* show time of stabilization of the hydraulic conductivity

types of hydraulic loading which produce large variations of hydraulic conductivity, two cumulative quantities are used. For characterizing the erosion process, the cumulative loss dry mass is computed: thanks to the optical sensor in the case of cohesive soils and by weighing the dry solid mass in each beaker of the effluent tank for cohesionless soils. Hydraulic loading is represented by the cumulative expended energy $E_{flow}(t)$ which is

Fig. 13 Erosion rate versus hydraulic shear stress, suffusion of cohesionless soils. *Black spots* show time of stabilization of the hydraulic conductivity

computed by time integration during the total duration t of the total flow power expressed by Eq. (6)

$$E_{\text{flow}}(t) = \sum_0^t P_{\text{flow}}(\Delta t)\Delta t \tag{11}$$

where $P_{\text{flow}}(\Delta t)$ is the total flow power for the duration Δt.

Loss dry mass and expended energy are two cumulative quantities which depend on the specimen volume and on the test duration. Thus, it is worth stressing to define the end of each test by the stabilization of the hydraulic conductivity. Figures 14 and 15 show the cumulative loss dry mass versus cumulative expended energy for cohesive soils and cohesionless soils, respectively.

For the size of tested specimens and the duration of realized tests, a large range of expended energy and a large range of cumulative loss mass are obtained at the end of tests: from 2×10^{-2} to 25.3 J and from 7.9×10^{-6} to 26.9 g, respectively (this last dry mass represents about 14 % of the total specimen mass).

According to these results, six categories of soil sensibility are proposed: from highly resistant to highly erodible, valid for both soil types, cohesive and cohesionless ones (cf. Figs. 16, 17). At the stabilization stage of the hydraulic conductivity or at the end of test in the case of the development of global backward erosion process, the position on the chart permits to determine the erodibility classification. It is worth noting that if the test is stopped before the stabilization of the hydraulic conductivity, the interpretation can lead to an overestimation of the soil resistance. Indeed, if we consider the mixture of kaolinite proclay and sand KPR25F75, for the suffusion tests performed under constant hydraulic gradient smaller than 10 (tests F14 and F15 in Fig. 16), the classification is between resistant and moderately resistant. However, for a higher applied hydraulic gradient or under flow rate-controlled conditions, the development of suffusion process finally leads to a global backward erosion of clayey sand, and the classification progresses from moderately resistant (see tests F10, F13, F17, F20 and F23 in Fig. 16) to erodible (see tests F10-
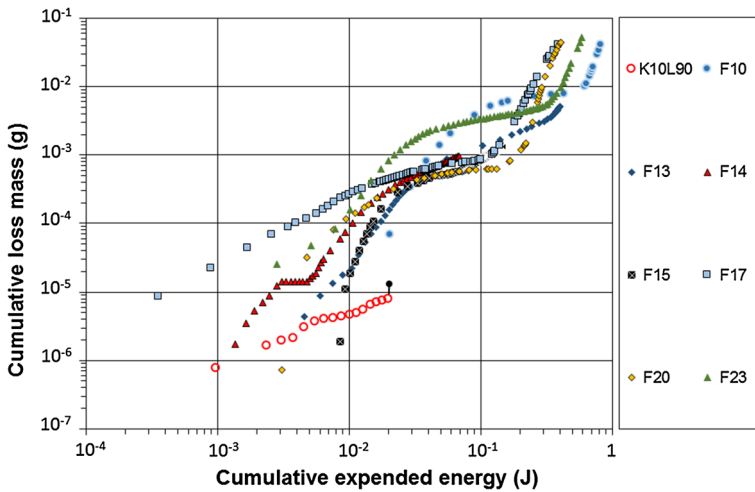
Fig. 14 Cumulative loss dry mass versus cumulative expended energy, cohesive soils. *Black spot* shows time of stabilization of the hydraulic conductivity
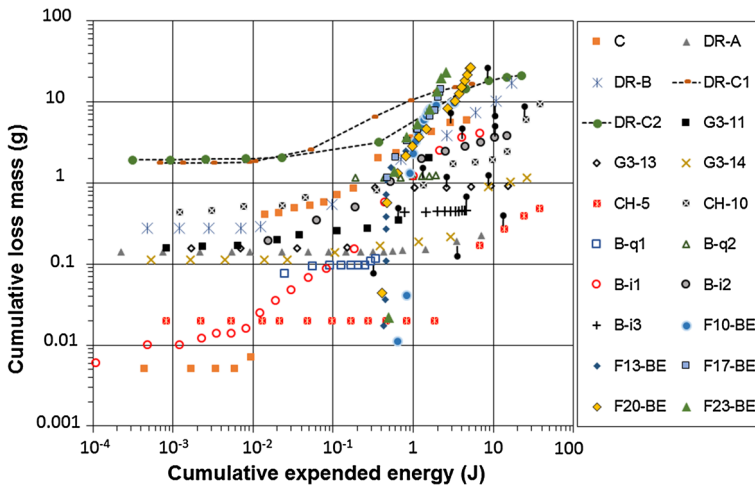

Fig. 15 Cumulative loss dry mass versus cumulative expended energy, suffusion of cohesionless soils and global backward erosion of clayey sand. *Black spots* show time of stabilization of the hydraulic conductivity

BE, F13-BE, F17-BE, F20-BE and F23-BE in Fig. 17). This remark shows the necessity to consider two conditions in order to perform suffusion test: (1) test must be realized since the stabilization of the hydraulic conductivity, and (2) under flow rate-controlled conditions or by increasing the applied hydraulic gradient in order to have the possibility to follow the development of all possible erosion processes.

According to this method, one specimen appears highly resistant: K10L90 (cf. Fig. 16). Further, two specimens can be classified as moderately resistant: CH5, DR-A (cf. Fig. 17). The classification of specimen G3-14 is between moderately resistant and moderately
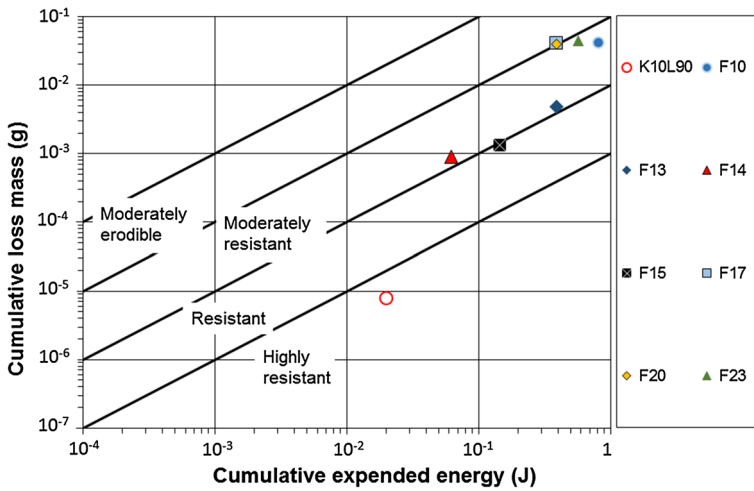
Fig. 16 Erodibility classification, suffusion of cohesive soils
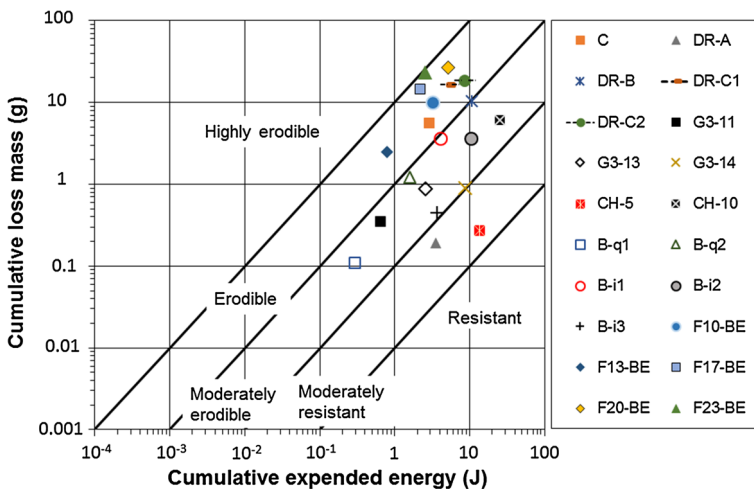
Fig. 17 Erodibility classification, suffusion of cohesionless soils and global backward erosion of clayey sand

erodible. Tests realized with soil B, under flow rate-controlled conditions (B-q1 and B-q2) or under hydraulic gradient-controlled conditions (B-i1, B-i2 and B-i3) permit to determine an identical classification as moderately erodible. The soils G3-11, G3-13 and CH10 can also be classified as moderately erodible, whereas the classification of specimen DR-B, appears between moderately erodible and erodible. For specimens C, DR-C1 and DR-C2, the classification is erodible.

The comparison of susceptibility classifications based on the less conservative criteria, with erodibility classification of tested soils, is displayed in Table 3. The erosion resistance index is also computed by Eq. (9) at the stabilization of the hydraulic conductivity or the

Table 3 Potential susceptibility classification based on the less conservative criteria, erosion resistance index and erodibility classification of soils tested

Soil reference in paper	Specimen reference in paper	Potential susceptibility	Erosion resistance index (−)	Erodibility classification
K10L90		U	6.40	HR
KPR25F75	F14	S	4.85	MR
	F15	S	5.03	R-MR
	F13	S	2.51	E
	F10	S	2.50	E
	F20	S	2.29	E
	F17	S	2.19	E
	F23	S	2.04	E
B	B-q1	S	3.43	ME
	B-q2	S	3.12	ME
	B-i1	S	3.05	ME
	B-i2	S	3.45	ME
	B-i3	S	3.91	ME
C		S	2.73	E
DR-A		S	4.27	MR
DR-B		U	3.02	ME-E
DR-C	C1	U	2.49	E
	C2	U	2.68	E
G3-11		U	3.29	ME
G3-13		U	3.46	ME
G3-14		U	3.98	MR-ME
CH-5		S-U	4.71	MR
CH-10		S-U	3.62	ME

S stable, *U* unstable, *HR* highly resistant, *R* resistant, *MR* moderately resistant, *ME* moderately erodible, *E* erodible

end of test in the case of the development of global backward erosion process (corresponding susceptibility categories: highly erodible for $I_\alpha < 2$; erodible for $2 \leq I_\alpha < 3$; moderately erodible for $3 \leq I_\alpha < 4$; moderately resistant for $4 \leq I_\alpha < 5$; resistant for $5 \leq I_\alpha < 6$; and highly resistant for $I_\alpha \geq 6$).

This comparison highlights that Chang and Zhang's criterion appears conservative for K10L90 as potential suffusion susceptibility of this clayey sand is unstable, whereas suffusion classification is highly resistant. Conversely, for clayey sand KPr25F75, this criterion leads to a classification as stable, and the suffusion test results show that erosion classification is erodible. This inability of criteria for assessing the right susceptibility of clayey sands can be due to the influence of the type of clay which is ignored by the grain size distribution criteria. For cohesionless soils B and C, the Chang and Zhang's criterion leads to susceptibility classification as stable, whereas the suffusion classification is moderately erodible and erodible, respectively. According to this criterion, the stability is correctly assessed if the value of gap ratio is smaller than 3. As the value of gap ratio is 2.5 for both tested soils, the authors suggest to re-evaluate the criterion by: $G_r < 2.5$.

5.7 Implications for engineering practice

According to the aforementioned results, a systematic method can be proposed. Two successive steps can be distinguished: the evaluation of the potential suffusion susceptibility and the erodibility classification.

According to the type of grain size distribution, the most successful criterion can be chosen between criteria from Chang and Zhang, Kenney and Lau or Wan and Fell.

When the evaluation of the susceptibility leads to potential instability, the erodibility characterization needs suffusion tests. Clay particles are made of flakes, and further, the different types of clay can be classified into eight categories. Among these, we should mention in particular the kaolinite group, the smectite group (mainly comprising of montmorillonite) and the illite group. Their structure and their differing chemical composition give them different particle sizes and a different sensitivity to erosion processes (Haghighi 2012). Thus, for plastic soils and particularly soils which contain illite or smectite clays, suffusion tests should be performed with water from the site, or with demineralized water. More generally, the test should be performed by increasing progressively the applied hydraulic gradient and it should be carried on until the hydraulic conductivity stabilizes.

With the objective to characterize independently the hydraulic loading and the induced erosion, the cumulative loss dry mass and the energy dissipated by the water seepage, E_{flow} are computed. Finally at the end of each test, which corresponds to the invariability of the hydraulic conductivity, the erosion sensibility classification can be evaluated by the position on the chart loss dry mass vs expended energy or by the value of erosion resistance index.

6 Conclusion

With the objective to evaluate the likelihood of suffusion initiation, several criteria based on the study of grain size distribution have been proposed in literature. The confrontation of the estimations obtained with the help of these grain size distribution criteria permits to identify three grain size distribution criteria that can be used in order to define the potential suffusion susceptibility. However, the confrontation has emphasized the limits of these criteria and the necessity to associate the analysis of the grain size distribution to the characterization of soil erodibility.

The characterization of soil susceptibility to suffusion requires suffusion tests and the interpretation of such tests is based on the evaluation of the generated load by the fluid flow. This evaluation is mainly carried out by expressing the critical value of the hydraulic gradient, the shear stress or the pore velocity. However, suffusion and filtration are two coupled processes that are governed by the geometry of the porous network, the physicochemical interactions between the solid phase and the fluid phase, as well as by the hydrodynamic conditions. In consequence, variations of both seepage velocity and hydraulic gradient (or pressure gradient) have to be taken into account to evaluate the hydraulic loading.

The interpretation based on rate of erosion of suffusion tests, realized under flow rate- or hydraulic gradient-controlled conditions, shows the necessity to take into account the history of hydraulic loading. A new interpretative method is proposed, linking the cumulative loss dry mass to the energy dissipated by the fluid flow. At the end of each test,

which corresponds to the invariability of the hydraulic conductivity, the energy-based method permits to determine the suffusion susceptibility for cohesionless materials and clayey sand. Characterization of the development of clayey sand backward erosion is also addressed by this method.

References

Bendahmane F, Marot D, Alexis A (2008) Experimental parametric study of suffusion and backward erosion. J Geotech Geoenviron Eng ASCE 134(1):57–67

Bonelli S, Marot D (2011) Micromechanical modelling of internal erosion. Eur J Environ Civil Eng 15(8):1207–1224

Briaud JL (2008) Case histories in soil and rock erosion: Woodrow Wilson Bridge, Brazos River Meander, Normandy Cliffs and New Orleans Levees. J Geotech Geoenviron Eng ASCE 134(10):1425–1447

Chang DS, Zhang LM (2013a) A stress-controlled erosion apparatus for studying internal erosion in soils. Geotech Test J 34(6):579–589

Chang DS, Zhang LM (2013b) Extended internal stability criteria for soils under seepage. Soils Found 53(4):569–583

Fell R, Fry JJ (eds) (2007) Internal erosion of dams and their foundations. Taylor & Francis, London

Fell R, Fry JJ (2013) State of the art on the likelihood of internal erosion of dams and levees by means of testing, chap 1. In: Bonelli S (ed) Erosion in geomechanics applied to dams and levees. ISTE—Wiley, London, pp 1–99

Fry JJ, Vogel A, Royet P, Courivaud JR (2012) Dam failures by erosion: lessons from ERINOH data bases. In: Proceedings of 6th international conference on scour and erosion (ICSE-6), 27–31 August, Paris, France, pp 273–280

Garner SJ, Fannin RJ (2010) Understanding internal erosion: a decade of research following a sinkhole event. Int J Hydropower Dams 17:93–98

Haghighi I (2012) Caractérisation des phénomènes d'érosion et de dispersion: développement d'essais et applications pratiques. Ph.D. Thesis. Université Paris-Est

Hanson GJ, Simon A (2001) Erodibility of cohesive streambeds in the loess area of the Midwestern, USA. Hydrol Process 15(1):23–38

Ke L, Takahashi A (2012) Strength reduction of cohesionless soil due to internal erosion induced by one dimensional upward seepage flow. Soils Found 52(2012):698–711

Kenney TC, Lau D (1985) Internal stability of granular filters. Can Geotech J 22:215–225

Kovacs G (1981) Seepage hydraulic. Elsevier, Amsterdam

Lafleur J (1999) Selection of geotextiles to filter broadly graded cohesionless soils. Geotext Geomembr 17:299–312

Lafleur J, Mlynarek J, Rollin AL (1989) Filtration of broadly graded cohesionless soils. J Geotech Eng 115(12):1747–1768

Li M, Fannin J (2008) Comparison of two criteria for internal stability of granular soil. Can Geotech J 45:1303–1309

Luo YL, Qiao L, Liu XX, Zhan ML, Sheng JC (2013) Hydro-mechanical experiments on suffusion under long-term large hydraulic heads. Nat Hazards 65:1361–1377

Marot D, Bendahmane F, Rosquoët F, Alexis A (2009) Internal flow effects on isotropic confined sand-clay mixtures. Soil Sediment Contam 18(3):294–306

Marot D, Regazzoni PL, Wahl T (2011a) Energy based method for providing soil surface erodibility rankings. J Geotech Geoenviron Eng ASCE 137(12):1290–1294

Marot D, Bendahmane F, Konrad JM (2011b) Multi-channel optical sensor to quantify particle stability under seepage flow. Can Geotech J 48:1772–1787

Marot D, Bendahmane F, Nguyen HH (2012) Influence of angularity of coarse fraction grains on internal erosion process. La Houille Blanche 6:47–53

Moffat R, Fannin J (2006) A large permeameter for study of internal stability in cohesionless soils. Geotech Test J 29(4):273–279

Moffat R, Fannin RJ, Garner SJ (2011) Spatial and temporal progression of internal erosion in cohesionless soil. Can Geotech J 48(3):399–412

Nguyen HH, Marot D, Bendahmane F (2012) Erodibility characterisation for suffusion process in cohesive soil by two types of hydraulic loading. La Houille Blanche 6:54–60

Reddi LN, Lee I, Bonala MVS (2000) Comparison of internal and surface erosion using flow pump test on a sand-kaolinite mixture. Geotech Test J 23(1):116–122

Sibille L, Lominé F, Poullain P, Sail Y, Marot D (2015a) Internal erosion in granular media: direct numerical simulations and energy interpretation. Hydrol Process 29(9):2149–2163. doi:10.1002/hyp.10351

Sibille L, Marot D, Sail Y (2015b) A description of internal erosion by suffusion and induced settlements on cohesionless granular matter. Acta Geotech 10:735–748. doi:10.1007/s11440-015-0388-6

Wan CF, Fell R (2004) Investigation of rate of erosion of soils in embankment dams. J Geotech Geoenviron Eng ASCE 130(4):373–380

Wan CF, Fell R (2008) Assessing the potential of internal instability and suffusion in embankment dams and their foundations. J Geotech Geoenviron Eng ASCE 134(3):401–407

Wörman A, Olafsdottir R (1992) Erosion in a granular medium interface. J Hydraul Res 30(5):639–655